

# Heptagon Amplitude in the Multi-Regge Regime

---

J. Bartels<sup>a</sup> V. Schomerus<sup>b</sup> M. Sprenger<sup>b</sup>

<sup>a</sup>*II. Institute Theoretical Physics,  
Hamburg University, Germany*

<sup>b</sup>*DESY Theory Group,  
Hamburg, Germany*

*E-mail:* [joachim.bartels@desy.de](mailto:joachim.bartels@desy.de), [volker.schomerus@desy.de](mailto:volker.schomerus@desy.de),  
[martin.sprenger@desy.de](mailto:martin.sprenger@desy.de)

ABSTRACT: As we have shown in previous work, the high energy limit of scattering amplitudes in  $\mathcal{N} = 4$  supersymmetric Yang-Mills theory corresponds to the infrared limit of the 1-dimensional quantum integrable system that solves minimal area problems in  $AdS_5$ . This insight can be developed into a systematic algorithm to compute the strong coupling limit of amplitudes in the multi-Regge regime through the solution of auxiliary Bethe Ansatz equations. We apply this procedure to compute the scattering amplitude for  $n = 7$  external gluons in different multi-Regge regions at infinite 't Hooft coupling. Our formulas are remarkably consistent with the expected form of 7-gluon Regge cut contributions in perturbative gauge theory. A full description of the general algorithm and a derivation of results will be given in a forthcoming paper.

KEYWORDS: AdS/CFT, gluon amplitudes, Regge limit, thermodynamic Bethe Ansatz

---

## Contents

<b>1</b>	<b>Introduction</b>	<b>1</b>
<b>2</b>	<b>Kinematics</b>	<b>2</b>
<b>3</b>	<b>Weak coupling</b>	<b>4</b>
<b>4</b>	<b>Strong coupling</b>	<b>6</b>
<b>5</b>	<b>Conclusion and Outlook</b>	<b>10</b>

---

## 1 Introduction

The solution of a 4-dimensional gauge theory remains a visionary dream of theoretical physics. Over the last years much progress has been made in the planar limit of  $\mathcal{N} = 4$  supersymmetric Yang-Mills theory (SYM). New methods based on symmetries and unitarity cuts have helped to re-organize perturbative computations e.g. of scattering amplitudes and have allowed to push them to previously unattainable orders, see for example [1] for the most recent results in this dynamical research area. Even with all this progress, however, the way from high to all orders still seems long and difficult. On the other hand, through the celebrated AdS/CFT correspondence, strongly coupled  $\mathcal{N} = 4$  SYM theory is related to superstring theory on  $AdS_5 \times S^5$  [2]. This duality severely constrains the strong coupling behavior of gauge theory amplitudes. Some of these constraints will be discussed below.

In gauge theories, scattering amplitudes in the high energy regime are of particular relevance. Remarkably, this regime is also computationally more accessible than generic kinematics. In fact, it has been known for a long time that integrable Heisenberg spin chains enter the expressions for scattering amplitudes in the so-called multi-Regge (high energy) limit [3, 4]. To leading logarithmic order, this is even true for QCD. Given these features of the multi-Regge limit in gauge theory one may wonder about the nature of the corresponding limit for string theory on  $AdS_5$ . In a previous paper we showed that the high energy limit for scattering amplitudes in  $\mathcal{N} = 4$  SYM corresponds to the infrared (low energy) limit of a 1-dimensional quantum integrable system for strings on  $AdS_5$  [5].

At strong coupling, scattering amplitudes in  $\mathcal{N} = 4$  SYM are believed to coincide with the area of a minimal 2-dimensional surface that approaches the boundary of  $AdS_5$  along a light-like polygon [6]. The latter encodes all the kinematic data of the process. This minimal area problem was shown to possess an intriguing reformulation in which the area is reproduced by the free energy of a 1-dimensional quantum integrable system [7, 8]. The particle content and interactions of the latter are designed so as to solve the original geometric minimal area problem. The 1-dimensional quantum system contains a number of

mass parameters and chemical potentials which matches precisely the number of kinematic invariants in the scattering process. For generic kinematics and particle densities of the 1-dimensional system one must solve a complicated system of coupled non-linear integral equations. These get replaced by a set of algebraic Bethe Ansatz equations in the infrared limit of the 1-dimensional system, i.e. when we enter the multi-Regge regime of gauge theory, see [9] for details.

The relations we have described in the previous paragraph allow us to find exact analytic results for scattering amplitudes in the multi-Regge regime of strongly coupled  $\mathcal{N} = 4$  SYM theory. Below we shall provide explicit expressions for  $n = 7$  external gluons. Let us recall that scattering amplitudes for  $n \leq 5$  external gluons are entirely fixed by dual conformal symmetry. A formula for  $n = 6$  was given recently in [10], see also [11]. The extensions to  $n = 7$  we shall describe below are new. Their detailed derivation will be given in our forthcoming paper [9].

The formulas we shall spell out below turn out to be very nicely consistent with the results of perturbative gauge theory at weak coupling. The latter will be discussed in section 3 before we present our expressions for the scattering amplitudes with  $n = 7$  external gluons in section 4. Section 2 contains some background information of kinematical invariants and the multi-Regge limit.

## 2 Kinematics

In this article we consider  $2 \rightarrow n - 2$  production amplitudes for massless external gluons. Our conventions for the enumeration of momenta is shown in figure 1. Given the  $n$  momenta  $p_1, \dots, p_n$  satisfying  $p_i^2 = 0$  we can build the following Mandelstam invariants

$$x_{ij}^2 = (p_{i+1} + \dots + p_j)^2, \quad (2.1)$$

where  $i, j = 1, \dots, n$ . These invariants are related by momentum conservation and Gram determinant relations so that only  $3n - 10$  of them are actually independent. Our description

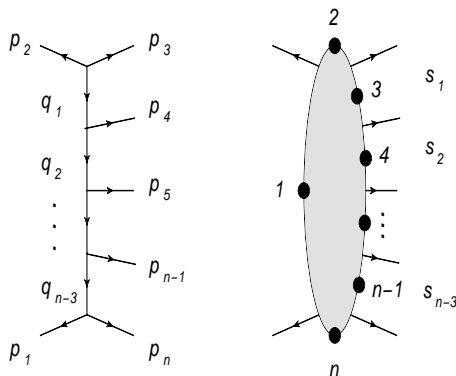


**Figure 1:** Kinematics of the scattering process  $2 \rightarrow n - 2$ . On the right-hand side we show a graphical representation of the dual variables  $x_i$ .

of scattering amplitudes below will be through the so-called remainder function  $R_n$ . The

latter depends on the kinematic invariants only through  $3n - 15$  dual conformally invariant cross ratios. For the discussion of the multi-Regge limit, the following choice is very useful:

$$u_{1\sigma} = \frac{x_{\sigma+1,\sigma+5}^2 x_{\sigma+2,\sigma+4}^2}{x_{\sigma+2,\sigma+5}^2 x_{\sigma+1,\sigma+4}^2}, \quad (2.2)$$

$$u_{2\sigma} = \frac{x_{\sigma+3,n}^2 x_{1,\sigma+2}^2}{x_{\sigma+2,n}^2 x_{1,\sigma+3}^2}, \quad (2.3)$$

$$u_{3\sigma} = \frac{x_{2,\sigma+3}^2 x_{1,\sigma+4}^2}{x_{2,\sigma+4}^2 x_{1,\sigma+3}^2}, \quad (2.4)$$

where  $\sigma = 1, \dots, n - 5$ . In the case of  $n = 6$  external gluons, there are only 3 independent cross ratios, which we shall simply denote by  $u_1, u_2, u_3$ . The number doubles when we go to  $n = 7$ .

In the multi-Regge limit, the cross ratios  $u_{1\sigma}$  tend to  $u_{1\sigma} \sim 1$  while the remaining ones tend to zero, i.e.  $u_{2\sigma}, u_{3\sigma} \sim 0$ . Cross ratios with the same index  $\sigma$  approach their limiting values such that the following reduced cross ratios remain finite

$$\left[ \frac{u_{2\sigma}}{1 - u_{1\sigma}} \right]^{\text{MRL}} =: \frac{1}{|1 + w_\sigma|^2}, \quad \left[ \frac{u_{3\sigma}}{1 - u_{1\sigma}} \right]^{\text{MRL}} =: \frac{|w_\sigma|^2}{|1 + w_\sigma|^2}. \quad (2.5)$$

Through these equations we have introduced the  $n - 5$  complex parameters  $w_\sigma$ .

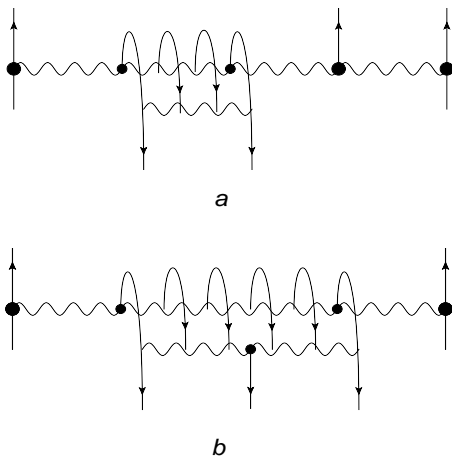


**Figure 2:** Graphical representation of two Regge regions of the 7-point amplitude.

An important aspect of the multi-Regge limit is the region in which it is actually performed. We consider  $2^{n-4}$  different regions which depend on the sign of the energies of the produced particles  $p_i^0$  for  $i = 4, \dots, n - 1$ . Different regions can be reached from the one in which all  $p_i^0$  are positive by analytic continuation. For  $n = 7$ , there are eight different regions which we label by  $(\nu_1 \nu_2 \nu_3)$  with  $\nu_i = \text{sgn}(p_{i+3})$ . The region  $(+++)$  is the original one in which all the  $p_i^0$  are positive. In this region, the multi-Regge limit of the remainder function vanishes [12]. The same is actually true for the three regions  $(-++), (+-+)$  and  $(+-)$ , which we therefore neglect in the following discussion. For the remaining four

regions, things are more interesting. Two of these regions are shown in figure 2. One of the missing regions in figure 2,  $(+ - -)$ , is related to  $(- - +)$  by a reflection along the vertical axis. For the strong coupling analysis we have to define paths of analytic continuation to connect the different regions. We choose to continue the 6 basic cross ratios along the following curves  $P_{\nu_1\nu_2\nu_3}$ :

$$\begin{aligned} P_{--+} : u_{11}(\varphi) &= e^{-2i\varphi} u_{11} \quad , \quad u_{12}(\varphi) = u_{12} \quad , \\ u_{21}(\varphi) &= u_{21} \quad , \quad u_{22}(\varphi) = e^{-i\varphi} u_{22} \quad , \\ u_{31}(\varphi) &= u_{31} \quad , \quad u_{32}(\varphi) = e^{i\varphi} u_{32} \quad , \end{aligned} \tag{2.6}$$

$$\begin{aligned} P_{---} : u_{1\sigma}(\varphi) &= e^{2i\varphi} (1 - \sqrt{1 - e^{-2i\varphi}}) u_{1\sigma} \quad , \\ u_{21}(\varphi) &= u_{21} \quad , \quad u_{22}(\varphi) = u_{22} \quad , \\ u_{31}(\varphi) &= u_{31} \quad , \quad u_{32}(\varphi) = u_{32} \quad , \end{aligned} \tag{2.7}$$

and

$$\begin{aligned} P_{-+-} : u_{11}(\varphi) &= e^{2i\varphi} u_{11} \quad , \quad u_{12}(\varphi) = e^{2i\varphi} u_{12} \quad , \\ u_{21}(\varphi) &= e^{-i\varphi} u_{21} \quad , \quad u_{22}(\varphi) = e^{i\varphi} u_{22} \quad , \\ u_{31}(\varphi) &= e^{i\varphi} u_{31} \quad , \quad u_{32}(\varphi) = e^{-i\varphi} u_{32} \quad . \end{aligned} \tag{2.8}$$

Here,  $\varphi \in [0, \pi]$  so that the cross ratios  $u_{1\sigma}(\varphi)$  come back to their starting values  $u_{1\sigma}$  at the endpoint of the path. The path  $P_{+--}$  is obtained from  $P_{--+}$  by the replacement  $u_{11} \leftrightarrow u_{12}$  and  $u_{2a} \leftrightarrow u_{3n-4-a}$ . These paths and their construction will be discussed in much more detail in our upcoming publication [9].

### 3 Weak coupling

We are now ready to discuss results on the multi-Regge limit of scattering amplitudes for  $n = 7$  gluons in perturbative gauge theory. Let us recall that in planar  $\mathcal{N} = 4$  super Yang-Mills theory the full color-ordered maximally helicity violating amplitude takes the following form

$$A_n \sim A_n^{(0)} e^{F_n^{\text{BDS}} + R_n} \quad .$$

Here,  $A_n^{(0)}$  is the tree level factor. The function  $F_n^{\text{BDS}}$  was introduced by Bern, Dixon and Smirnov in [13]. It contains the known singular terms of the amplitudes along with a relatively simple finite term. It captures the amplitude correctly at one loop but misses important contributions starting from two loops. The so-called remainder function  $R_n$  is IR-finite and invariant under dual conformal transformations, i.e. it is a function of the  $3n - 15$  cross ratios introduced above. While  $R_n$  vanishes for  $n = 4, 5$ , it must be non-zero starting from  $n = 6$  in order to correct the unphysical analytical structure of the BDS Ansatz, see [12].

The full remainder function  $R_n$  was bootstrapped for  $n = 6$  up to four loops [14–17] and its symbol is known for  $n > 6$  at two loops [18]. There exist further results for very

special kinematics, but these are not relevant for our discussion. The most important results concern the multi-Regge regime in which the cross ratios tend to the limit values described above. Since the remainder function contains branch cuts, its limiting behavior depends on the multi-Regge region we consider. In fact, if we perform this limit in the region where all  $p_i^0 > 0$ , then the limit of the remainder function is trivial. In order to take the limit in other regions, we must continue the cross ratios. For  $n = 7$  gluons, the regions of interest are  $(- - +)$ ,  $(- - -)$  and  $(- + -)$ . In all three cases the limiting behavior of the remainder function  $R_7$  is described by a factorizing ansatz. For the region  $(- - +)$  this takes the form

$$\begin{aligned} \left[ e^{R_7 + i\pi\delta_7} \right]_{---+}^{\text{MRL}} &= i\frac{\lambda}{2} \sum_{n_1=-\infty}^{\infty} (-1)^{n_1} \int_{-\infty}^{\infty} \frac{d\nu_1}{2\pi} |\Phi(\nu_1, n_1)|^2 \\ &\times |w_1|^{2i\nu_1} e^{-in_1\phi_1} \left( (1 - u_{11}) \frac{|w_1|}{|1 + w_1|^2} \right)^{-\omega(\nu_1, n_1)} + \dots \end{aligned} \quad (3.1)$$

Here, the phase  $\delta_7$  denotes contributions from the analytic continuation of  $F_7^{\text{BDS}}$ , the impact factor  $\Phi$  is given by an expansion in powers of the coupling (known up to N<sup>3</sup>LO), and the BFKL eigenvalues  $\omega(\nu, n)$  are the lowest eigenvalues of a non-compact  $\text{SL}(2, \mathbb{C})$  Heisenberg Hamiltonian for a spin chain of length two, see [19]. The parameters  $\nu, n$  label irreducible representations of  $\text{SL}(2, \mathbb{C})$ . Explicit expression for  $\omega(\nu, n)$  may be found in [17, 20, 21]. Finally, the dots indicate that in addition to the Regge cut contribution there is still a conformally invariant Regge pole term which, in the present context, is not of interest.

One may expect that the corresponding result for the second region is a bit more complicated. This is indeed the case. For the region  $(- - -)$  one finds,

$$\begin{aligned} \left[ e^{R_7 + i\pi\delta_7} \right]_{----}^{\text{MRL}} &= i\frac{\lambda}{2} \sum_{n_1, n_2} (-1)^{n_1 + n_2} \int \int \frac{d\nu_1 d\nu_2}{(2\pi)^2} \Phi(\nu_1, n_1)^* C(\nu_1, n_1; \nu_2, n_2) \Phi(\nu_2, n_2) \\ &\times \prod_{\sigma=1}^2 |w_\sigma|^{2i\nu_\sigma} e^{-in_\sigma\phi_\sigma} \left( (1 - u_{1\sigma}) \frac{|w_\sigma|}{|1 + w_\sigma|^2} \right)^{-\omega(\nu_\sigma, n_\sigma)} + \dots \end{aligned} \quad (3.2)$$

The impact factors  $\Phi$  and BFKL eigenvalues  $\omega$  are the same as in eq.(3.1). The new production vertex  $C$  has been calculated to LO in eqs.(19), (20) of [22]. The leading order momentum space expression for the production vertex is real-valued, whereas the next-to leading order correction is expected to acquire a phase. Eq.(3.2) represents the leading contribution of this path, but is not the full weak coupling result (as indicated by the dots). Namely, in addition to the given integral, the remainder function contains a conformal Regge pole contribution and two subtraction terms. In addition, we have to subtract the one loop terms from the two energy factors in the second line of eq.(3.2). The complete weak coupling result is given in [23, 24]. While these terms are relevant for any comparison with a loop expansion of the 7-point amplitudes, in our discussion it is sufficient to use eq.(3.2).

Finally, for the region  $(- + -)$ , the leading order result is of the same form as eq.(3.2): Differences between the two regions are expected to appear at NLO where the production vertex becomes complex-valued. For the region  $(- + -)$  the production vertex is expected to

be the complex conjugate of the one for the previous region (---). Also, the subtraction terms (indicated in eq.(3.2) by the dots) are different from those of the region (---).

It is important to note that, apart from the production vertex  $C$ , these expressions for the 7-point remainder functions are determined by functions which appear already in the 6-point remainder functions, in particular the eigenvalue function  $\omega(\nu, n)$ . This does not mean that the  $n = 6$  gluon results determine the multi-Regge limit of the remainder functions  $R_n$  for  $n \geq 7$ . In fact, already at  $n = 8$  gluons there exist kinematic regions in which a new function appears. This is related to the fact that the continuation along certain paths starts to probe eigenvalues  $\omega_3(\nu_1, n_1, \nu_2, n_2)$  of an open Heisenberg spin chain with three sites. One of the remarkable outcomes of our analysis is that the close relation between 6- and 7-point high energy amplitudes is also present at strong coupling.

## 4 Strong coupling

Let us now come to the main new results of this work, namely the computation of remainder functions in the multi-Regge regime of strongly coupled  $\mathcal{N} = 4$  SYM theory. In particular, we shall spell out formulas for the remainder function with  $n = 7$  external gluons.

As we briefly reviewed in the introduction, in strongly coupled  $\mathcal{N} = 4$  SYM theory scattering may be reformulated as a minimal area problem. The latter possesses an intriguing mathematical reformulation through a 1-dimensional quantum integrable system which is composed of particles whose interaction is fully characterized through  $2 \mapsto 2$  scattering phases. This system possesses  $3n - 15$  external parameters which can be thought of as masses and chemical potentials. Given any such system one needs to determine self-consistently the rapidity densities of the various particles as a function of the external parameters. This is done by solving a system of coupled non-linear integral equations which involve both the external parameters and the scattering phases. Roughly, such equations take the form

$$\log Y(\theta) = -m \cosh \theta + C + \int_{-\infty}^{\infty} d\theta' K(\theta - \theta') \log(1 + Y(\theta')) . \quad (4.1)$$

Here we have suppressed all the indices that run over the various particles for simplicity. The parameters  $m$  and  $C$  play the role of the mass parameter and chemical potential, respectively, and

$$-2\pi i K(\theta) =: \partial_\theta \log S(\theta) \quad (4.2)$$

is associated with the scattering phase  $S(\theta)$ . Once the densities  $Y$  have been found, they can be used to determine the total energy of the system.

There are two rather important observations concerning non-linear integral equations of the form (4.1). The first one addresses their behavior under analytic continuation of the parameters  $m$  and  $C$ . As we move the parameters through the complex plane, the solution  $Y(\theta)$  to the integral equations changes. In particular, the solutions of the equation  $Y(\theta_*) = -1$  will wander through the space of complex rapidities  $\theta$ . Looking at eq.(4.1) we can see that solutions of  $Y(\theta_*) = -1$  are associated with poles in the integrand of the

non-linear integral equation. When these poles cross the integration contour, the equation picks up a residue contribution and hence assumes the new form

$$\log Y(\theta) = -m' \cosh \theta + C' + \sum_i \sigma_i \log S(\theta - \theta_i) + \int_{-\infty}^{\infty} d\theta' K(\theta - \theta') \log(1 + Y(\theta')) \quad (4.3)$$

with sign factors  $\sigma_i$  depending on whether the solution  $\theta_i$  of  $Y(\theta_i) = -1$  crosses from the lower half of the complex plane into the upper half or vice versa. Whenever such a crossing takes place, a new contribution to the total energy of the system appears. One may interpret these changes to the system as excitations that have been produced while we continued the system parameters  $m$  and  $C$  to the values  $m'$  and  $C'$ .

The second important observation concerning eq.(4.1) addresses its behavior in the limit of large mass parameter  $m$ . To be more precise, the parameter  $m$  is dimensionless and should rather be thought of as a product  $m = ML$  of a physical mass  $M$  and the system size  $L$ . Sending  $m$  to infinity is then achieved by making the physical mass  $M$  large or by going to the limit of large system size. In such a limit, the first term on the right-hand side (4.1) goes to minus infinity and hence the function  $Y(\theta)$  that appears in the logarithm on the left-hand side must approach zero. This in turn implies that  $\log(1 + Y(\theta')) \sim 0$ . Thus we can neglect the integral on the right-hand side of our non-linear integral equations. We are therefore left with the first two terms on the right-hand side of eq.(4.3). If we evaluate this equation at the points  $\theta = \theta_j$ , use that  $Y(\theta_j) = -1$  and exponentiate we obtain a set of algebraic Bethe Ansatz equations,

$$e^{m' \cosh \theta_j - C'} = \prod_{i \neq j} S^{\sigma_i}(\theta_j - \theta_i).$$

These can be solved for the rapidities  $\theta_j$  of the excitations. Once they have been determined we can compute the energy as a sum of energies, one for each crossed solution of  $Y(\theta_i) = -1$ .

All this applies to the minimal area problem in  $AdS_5$ . In that case there exist  $n - 5$  complex mass parameters  $m_s$  and  $n - 5$  purely complex chemical potential  $C_s$ . When the  $m_s$  are sent to infinity in a certain direction of the complex plane such that

$$m_s e^{i(s-1)\frac{\pi}{4}} \rightarrow \infty + i \log v_s \quad (4.4)$$

with both  $C_s$  and  $v_s$  fixed and real, then the cross ratios of the process approach the multi-Regge regime [5]. The limit is parametrized by  $n - 5$  complex variables  $w_\sigma = w_\sigma(v_s, C_s)$  (cf. eq.(2.5)) that can be scanned by adjusting  $v_s$  and  $C_s$ .

In the large volume limit (4.4), the energy of the 1-dimensional quantum system vanishes and this in turn implies that the remainder function vanishes in multi-Regge kinematics of strongly coupled  $\mathcal{N} = 4$  SYM theory, as long as we are in the region with all  $p_i^0$  positive. This is the same behavior as in the weakly coupled theory. In order to obtain a non-vanishing result, we need to continue into another multi-Regge region, as we discussed in the previous sections. This analytic continuation has to be performed before neglecting the integrals in eq.(4.1) since poles can cross the integration contour during the continuation, as explained before. We have worked this out for a number of examples. Since the



system parameters of the 1-dimensional quantum system are related to the cross ratios, we must continue  $m_s$  and  $C_s$  along appropriate paths.

Let us now describe all this in a bit more detail for the case of  $n = 7$  gluons and the region  $(- - +)$  we depict in figure 2a. In terms of the system parameters  $m_s$  and  $C_s$ ,  $s = 1, 2$ , the path  $P_{--+}$  takes the form shown in figure 3. Our findings are described and commented in the captions <sup>1</sup>.

Once these curves are known, we can watch the position of the solutions to  $Y(\theta_*) = -1$  to see whether they cross the real axis. In the case of 7 external gluons, there are actually six  $Y$ -functions which we label by  $Y_{as}$  with  $a = 1, 2, 3$  and  $s = 1, 2$ . Figure 4 displays how the solutions of  $Y_{as}(\theta_*) = -1$  move as we vary the system parameters along the paths of figure 3. We see that a pair of solutions cross the real axis. The excitations that are created in this process possess non-vanishing energy which can be computed analytically and contributes to the following final expression for the remainder function<sup>2</sup>

$$R_{7,--\pm}^{\infty \text{MRL}} + i\pi\delta_{7,--\pm} = \mathcal{R}^{\infty}(u_{a1}) ,$$

where

$$\mathcal{R}^{\infty}(u_1, u_2, u_3) = \frac{\sqrt{\lambda}}{2\pi} e_2 \ln(1 - u_1) + \frac{\sqrt{\lambda}}{2\pi} e_2 \left( \frac{1}{2} \ln |w|^2 - \ln |1 + w|^2 \right) \quad (4.5)$$

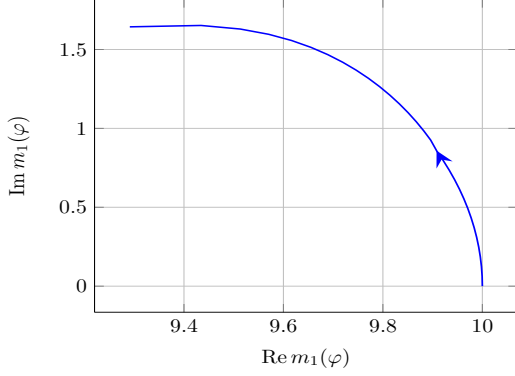
and  $e_2 = -\sqrt{2} + \frac{1}{2} \ln(3 + 2\sqrt{2})$ . This function is the same that was found previously in the investigation of 6-gluon scattering amplitudes [10]. Note however, that the various individual contributions to the remainder function must conspire in order to produce this answer. Of course, one may carry out the same analysis for the path  $P_{+--}$  in order to find

$$R_{7,+--}^{\infty \text{MRL}} + i\pi\delta_{7,+--} = \mathcal{R}^{\infty}(u_{a2}) .$$

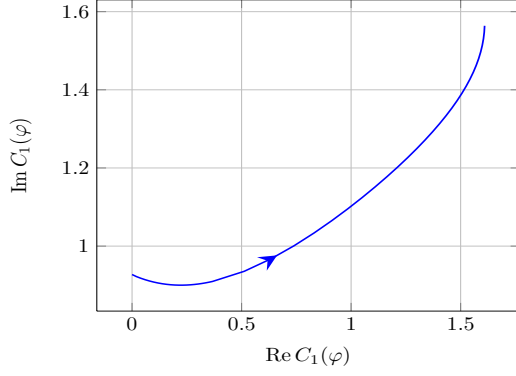
Let us now turn to the most interesting case, namely the path  $P_{---}$ . The relevant curves for the mass parameters  $m_s$  and the chemical potentials  $C_s$  are shown in figure 5. For simplicity we have chosen symmetric initial conditions  $m_1 = m_2 = m$  and  $C_1 = -C_2 = C$ . Since the path  $P_{---}$  respects this symmetry, the equalities remain true for all values of the continuation parameter  $\varphi$ . When we drive the system parameters along these paths, four solutions of  $Y_{as}(\theta_*) = -1$  cross the real axis. For  $Y_{12}$  their paths are shown in figure 6a. The other two poles are contributed by  $Y_{31}$ . The numerical work underlying these plots turned out to be much more intricate than for the hexagon. In particular, it is quite challenging to determine the positions of  $\theta_*$  at the end of the continuation from the numerics. It turns out that for very large masses  $m_s$  the position of these solutions is  $\theta_* = \pm i\pi/4$ , independently of the precise values of the remaining parameters. But the approach to these final positions requires extremely high masses, see figure 6b. Fortunately, the positions can once again be found analytically, as will be explained in our forthcoming paper [9]. The final formula for

<sup>1</sup>It should be pointed out that there is shift in the indices of the variables: for our path  $P_{--\pm}$  the triplet  $u_{a\sigma}$  with  $\sigma = 1$  appears in our final result. However, due to conventions of labeling the functions  $Y_{as}$ , the corresponding parameters  $m_s$  and  $C_s$  carry the label  $s = 2$ .

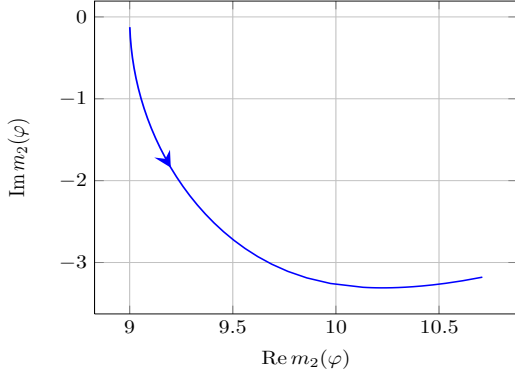
<sup>2</sup>Note that contrary to our previous publications we define the remainder function at strong coupling including the factor  $-\frac{\sqrt{\lambda}}{2\pi}$  for better comparison with the weak coupling results.



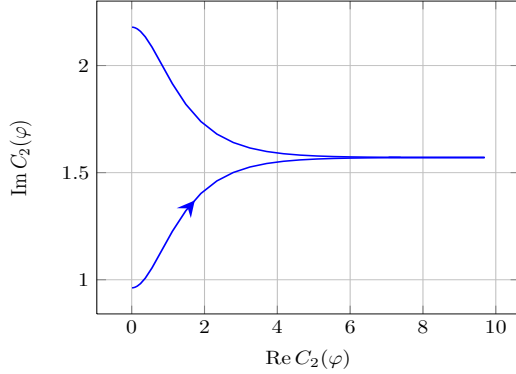
(a) Path of the system parameter  $m_1$ . Note that the absolute value of  $m_1$  remains large throughout the continuation.



(b) Path of the system parameter  $C_1$ . Note that  $C_1$  undergoes only small changes when compared with those seen in  $C_2$ .



(c) Path of the system parameter  $m_2$ . Note that the absolute value of  $m_2$  remains large throughout the continuation.



(d) Path of the system parameter  $C_2$ . Note that  $C_2$  is very strongly peaked near  $\varphi = \pi/2$ .

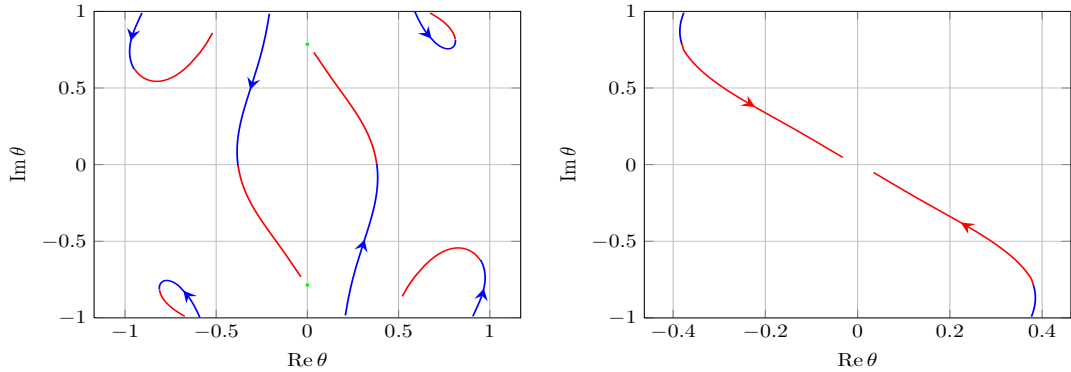
**Figure 3:** In order to describe the path  $P_{-+}$  we vary the system parameters  $m_1, m_2$  and  $C_1, C_2$  along the curves shown above. As start values we choose  $m_1(0) = 10, m_2(0) = 9$  and  $C_1(0) \sim .93i, C_2(0) = .96i$ . These values determine the values of the kinematic variables  $w_i$ . The qualitative features of the curves do not depend on the precise values of the initial conditions. Note that the curves for  $m_2$  and  $C_2$  are very similar to those of  $m$  and  $C$  found in the case of 6-gluon scattering, see [11].

the resulting remainder function is

$$R_{7,----}^{\infty \text{MRL}} + i\pi\delta_{7,----} = \mathcal{R}^{\infty}(u_{a1}) + \mathcal{R}^{\infty}(u_{a2}) . \quad (4.6)$$

As in the previous two cases, the expression for the remainder function in the strongly coupled theory is built from the same function  $\mathcal{R}^{\infty}$  that describes the high energy scattering of 6 gluons. This is in perfect agreement with the weak coupling expansion in eq.(3.2).

There is one curve left to discuss, namely  $P_{-+-}$ . In this case it turns out that none of the solutions of  $Y_{as}(\theta_*) = -1$  actually cross the real axis. Hence, no excitation is produced



(a) As we continue along the path  $P_{--+}$ , two solutions of the equation  $Y_{32}(\theta_*) = -1$  cross the real axis. The green dots indicate the analytically determined endpoints of the crossed solutions.

(b) As we continue along the path  $P_{--+}$  two solutions of  $Y_{22}(\theta_*) = -1$  approach the real axis towards the end of the continuation.

**Figure 4:** During the continuation along  $P_{--+}$  some solutions of  $Y_{as}(\theta_*) = -1$  approach or cross the real line. These are shown in the plots. We change the color of the plot once the pair of solutions crosses the real axis. Solutions of  $Y_{a1}(\theta_*) = -1$  move very little and stay away from the real axis. This is related to the small changes we see in the parameter  $C_1$ , see figure 3b. The pattern of pole crossings is very similar to that found for 6-gluon scattering, see [11].

so that the remainder function remains at

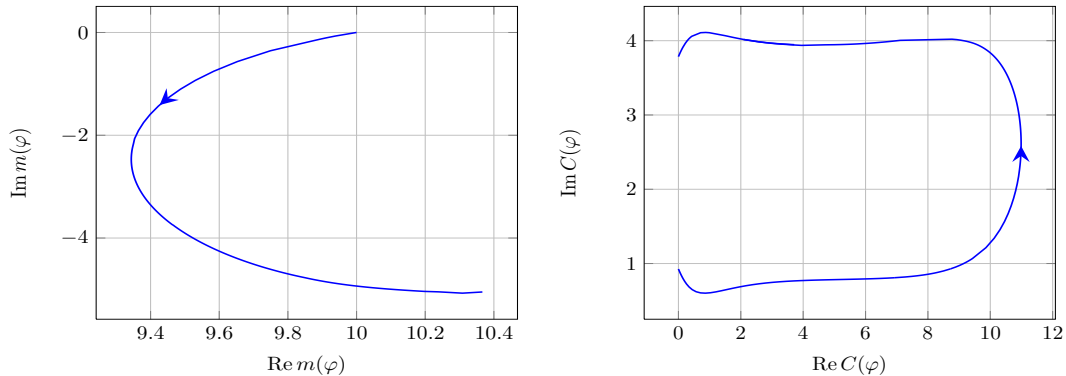
$$R_{7,-+-}^{\infty, \text{MRL}} + i\pi\delta_{7,-+-} = 0, \quad (4.7)$$

just as in the Euclidean region, except for the appearance of a phase. The corresponding analysis at weak coupling shows the presence of the Regge cut in the kinematic region  $(-+-)$ , but there remains the possibility that our path of analytic continuation,  $P_{--+}$ , needs to be modified. It is certainly important to clarify this issue.

## 5 Conclusion and Outlook

In this note we have reported the results we obtain for the multi-Regge limit of 7-gluon scattering amplitudes in strongly coupled  $\mathcal{N} = 4$  SYM theory. These are obtained through a very general algorithm that can in principle produce similar formulas for any number of external gluons. The general procedure and the technical details that lead to our results for 7 gluons are discussed in a forthcoming publication [9].

There are several interesting directions to pursue. As we have mentioned already, the choice of the path  $P_{--+}$  should be studied carefully, in order to see whether results in the weakly coupled theory are compatible with what we found for strong coupling. Let us also note that all our analysis is performed for finite values of the parameters  $w_\sigma$ . When we send one or several of these parameters to zero, some key features of the various plots we produced



(a) Path of the system parameter  $m = m_1 = m_2$ . Note that the absolute value of  $m$  remains large throughout the continuation.

(b) Path of the system parameter  $C = C_1 = -C_2$ . Note that  $C$  becomes large (of the order of the mass) again, but it is not strongly peaked.

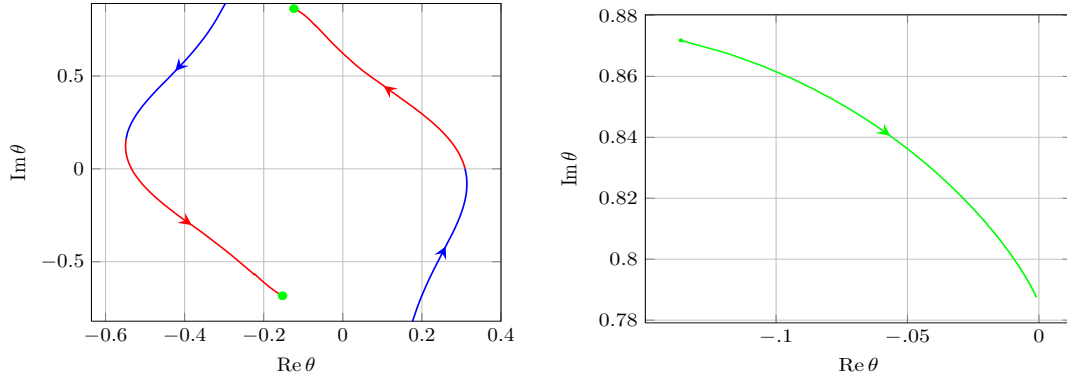
**Figure 5:** In order to describe the path  $P_{---$  we vary the system parameters  $m_s$  and  $C_s$  along the curves shown in this figure. For these figures we have chosen symmetric initial conditions  $m(0) = m_1(0) = m_2(0) = 10$  and  $C(0) = C_1(0) = -C_2(0) \sim .93i$ . For other (non-symmetric) initial conditions the qualitative features of these curves remain the same. Initial conditions must be varied in order to explore the whole range of dynamical variables  $w_1$  and  $w_2$ .

numerically could change. So, it may not be correct to simply take our expressions for the remainder function and evaluate them in the collinear limit  $w_\sigma = 0$ . The issue certainly requires further attention, in particular in view of the close connection between the Wilson loop OPE, see [25–27] and references therein, and the collinear expansion of the multi-Regge results for 6-gluon amplitudes in the weakly coupled theory [28].

**Acknowledgments:** We would like to thank Benjamin Basso, Simon Caron-Huot, Lance Dixon, Andrey Kormilitzin, Jan Kotanski, Lev Lipatov, Lionel Mason and David Skinner for useful discussions. This work was supported by the SFB 676. The research leading to these results has also received funding from the People Programme (Marie Curie Actions) of the European Union’s Seventh Framework Programme FP7/2007-2013/ under REA Grant Agreement No 317089 (GATIS).

## References

- [1] see <http://wwwth.mpp.mpg.de/members/strings/amplitudes2013/amplitudes.html>
- [2] J. M. Maldacena, *The Large  $N$  limit of superconformal field theories and supergravity*, Adv. Theor. Math. Phys. **2** (1998) 231 [hep-th/9711200].
- [3] L. N. Lipatov, *High-energy asymptotics of multicolor QCD and exactly solvable lattice models*, [hep-th/9311037].
- [4] L. D. Faddeev and G. P. Korchemsky, *High-energy QCD as a completely integrable model*, Phys. Lett. B **342** (1995) 311 [hep-th/9404173].



(a) As we continue along the path  $P_{---}$ , two of the solutions to  $Y_{12}(\theta_*) = -1$  cross the real axis. Note that the crossing happens at two different values of the continuation parameter  $\varphi$ . The first pole crossing is correlated with the change of colors from blue to red.

(b) The end-point of the right curve in figure 6a depends on the initial value of  $m = m_1 = m_2$ . Our figure shows its position as a function of  $m$  in a range between  $m = 10$  and  $m = 2000$ . Note that for very large values of  $m$ , our numerical results approaches the analytic value  $\theta_* = i\pi/4$ .

**Figure 6:** Four solutions of the equations  $Y_{as}(\theta_*) = -1$  cross the real axis while we continue along  $P_{---}$ . We have displayed the relevant solutions for  $Y_{12}$ . The corresponding figure for  $Y_{31}$  looks very similar. For all other  $Y$  functions, the solutions do not get close to the real axis. The final position of the solutions at  $\varphi = \pi$  determines the free energy. Note that this value is approached very slowly as we crank up the mass parameter  $m$ .

- [5] J. Bartels, V. Schomerus and M. Sprenger, *Multi-Regge Limit of the n-Gluon Bubble Ansatz*, JHEP **1211** (2012) 145 [arXiv:1207.4204 [hep-th]].
- [6] L. F. Alday and J. M. Maldacena, *Gluon scattering amplitudes at strong coupling*, JHEP **0706** (2007) 064 [arXiv:0705.0303 [hep-th]].
- [7] L. F. Alday, D. Gaiotto and J. Maldacena, *Thermodynamic Bubble Ansatz*, JHEP **1109** (2011) 032 [arXiv:0911.4708 [hep-th]].
- [8] L. F. Alday, J. Maldacena, A. Sever and P. Vieira, *Y-system for Scattering Amplitudes*, J. Phys. A **43** (2010) 485401 [arXiv:1002.2459 [hep-th]].
- [9] J. Bartels, V. Schomerus and M. Sprenger, in preparation.
- [10] J. Bartels, J. Kotanski, V. Schomerus and M. Sprenger, *The Excited Hexagon Reloaded*, arXiv:1311.1512 [hep-th].
- [11] J. Bartels, J. Kotanski and V. Schomerus, *Excited Hexagon Wilson Loops for Strongly Coupled  $N=4$  SYM*, JHEP **1101** (2011) 096 [arXiv:1009.3938 [hep-th]].
- [12] J. Bartels, L. N. Lipatov and A. Sabio Vera, *BFKL Pomeron, Reggeized gluons and Bern-Dixon-Smirnov amplitudes*, Phys. Rev. D **80** (2009) 045002 [arXiv:0802.2065 [hep-th]].
- [13] Z. Bern, L. J. Dixon and V. A. Smirnov, *Iteration of planar amplitudes in maximally supersymmetric Yang-Mills theory at three loops and beyond*, Phys. Rev. D **72** (2005) 085001 [hep-th/0505205].
- [14] A. B. Goncharov, M. Spradlin, C. Vergu and A. Volovich, *Classical Polylogarithms for*

- Amplitudes and Wilson Loops*, Phys. Rev. Lett. **105** (2010) 151605 [arXiv:1006.5703 [hep-th]].
- [15] L. J. Dixon, J. M. Drummond and J. M. Henn, *Bootstrapping the three-loop hexagon*, JHEP **1111** (2011) 023 [arXiv:1108.4461 [hep-th]].
- [16] L. J. Dixon, J. M. Drummond, M. von Hippel and J. Pennington, *Hexagon functions and the three-loop remainder function*, JHEP **1312** (2013) 049 [arXiv:1308.2276 [hep-th]].
- [17] L. J. Dixon, J. M. Drummond, C. Duhr and J. Pennington, *The four-loop remainder function and multi-Regge behavior at NNLLA in planar  $N=4$  super-Yang-Mills theory*, arXiv:1402.3300 [hep-th].
- [18] S. Caron-Huot, *Superconformal symmetry and two-loop amplitudes in planar  $N=4$  super Yang-Mills*, JHEP **1112** (2011) 066 [arXiv:1105.5606 [hep-th]].
- [19] L. N. Lipatov, *Integrability of scattering amplitudes in  $N=4$  SUSY*, J. Phys. A **42** (2009) 304020 [arXiv:0902.1444 [hep-th]].
- [20] J. Bartels, L. N. Lipatov and A. Sabio Vera,  *$N=4$  supersymmetric Yang Mills scattering amplitudes at high energies: The Regge cut contribution*, Eur. Phys. J. C **65** (2010) 587 [arXiv:0807.0894 [hep-th]].
- [21] V. S. Fadin and L. N. Lipatov, *BFKL equation for the adjoint representation of the gauge group in the next-to-leading approximation at  $N=4$  SUSY*, Phys. Lett. B **706** (2012) 470 [arXiv:1111.0782 [hep-th]].
- [22] J. Bartels, A. Kormilitzin, L. N. Lipatov and A. Prygarin, *BFKL approach and  $2 \rightarrow 5$  maximally helicity violating amplitude in  $\mathcal{N} = 4$  super-Yang-Mills theory*, Phys. Rev. D **86** (2012) 065026 [arXiv:1112.6366 [hep-th]].
- [23] J. Bartels, A. Kormilitzin and L. Lipatov, *Analytic structure of the  $n = 7$  scattering amplitude in  $\mathcal{N} = 4$  SYM theory at multi-Regge kinematics: Conformal Regge Pole Contribution*, arXiv:1311.2061 [hep-th].
- [24] J. Bartels, A. Kormilitzin and L. Lipatov, in preparation.
- [25] B. Basso, A. Sever and P. Vieira, *Spacetime and Flux Tube S-Matrices at Finite Coupling for  $N=4$  Supersymmetric Yang-Mills Theory*, Phys. Rev. Lett. **111** (2013) 9, 091602 [arXiv:1303.1396 [hep-th]].
- [26] B. Basso, A. Sever and P. Vieira, *Space-time S-matrix and Flux tube S-matrix II. Extracting and Matching Data*, JHEP **1401** (2014) 008 [arXiv:1306.2058 [hep-th]].
- [27] B. Basso, A. Sever and P. Vieira, *Space-time S-matrix and Flux-tube S-matrix III. The two-particle contributions*, arXiv:1402.3307 [hep-th].
- [28] Y. Hatsuda, *Wilson loop OPE, analytic continuation and multi-Regge limit*, arXiv:1404.6506 [hep-th].